



# Proapoptotic and anti-angiogenic activity of (2E)-3-(2-bromo-6-hydroxy-4-methoxyphenyl)-1-(naphthalene-2-yl)prop-2-en-1-one in MCF7 cell line

Dileep Kumar M. Guruswamy<sup>1</sup> · Shankar Jayarama<sup>1</sup>

Received: 13 September 2019 / Accepted: 5 January 2020 / Published online: 29 January 2020  
© Institute of Chemistry, Slovak Academy of Sciences 2020

## Abstract

In the present study, synthesized the d1 by the Claisen–Schmidt condensation method and the resultant compound was characterized by <sup>1</sup>H NMR and <sup>13</sup>C NMR spectral studies. Compound d1 exhibits incredible anticancer movement on MCF7 with the IC<sub>50</sub> estimations of 6.555–10.14 μM. The further apoptotic-related examination has been finished for the expression level of Caspase 9 and Caspase 3. Supporting this, we overview the in vivo adversary of tumor development and anti-angiogenic action of d1 in Ehrlich Ascites Carcinoma (EAC). The d1 treatment inhibited the tumor development and expanded the life expectancy of the EAC-bearing mice without appearing symptoms on healthy mice, as uncovered by histological parameters. The apoptosis induced in the early apoptotic phase and Caspase activation at a specified concentration showed significant apoptotic activity. In vivo models in EAC for anti-angiogenic models also showed promising activity at a specified concentration. The present study revealed that the d1 showed significant tumor-inhibiting capabilities even in lesser concentrations in both in vitro as well as in vivo suggested that our d1 as a potent anticancer drug.

**Keywords** Naphthalene chalcones · Caspase 3 · VEGF · H&E, BAX, Bcl2

## Introduction

Cancerous growth is one in all the most medical problems within the human population and one of the numerous reasons for death. A little of the ordinarily occurring compounds are progressively keen on malignant tumor medications in numerous human malignant growth (Partridge et al. 2016; Newman and Cragg 2016; Cragg and Newman 2013; Mishra and Tiwari 2011; Rodrigues et al. 2016a, b). Chalcones are present flavonoid compounds that act as chemotherapeutic agents attributable to their biological activity. Thus, we glance to synthesize new molecules from the plant origin (Warmka et al. 2012). Structurally, chalcones include an aliphatic three-carbon chain that links two aromatic rings. Chalcones, or 1, 3-disubstituted-prop-2-en-1-ones (R1COCH=CHR2), are α, β-unsaturated ketones consisting of two aromatics having a diverse array of substituents and

that they classified mutually of the vital subgroups of flavonoids, and its scaffolds displaying distinctive medicative and biological properties. Chalcones are benzyl group acetophenone or benzylideneacetophenone, and their rings are interconnected by extremely natural action three carbon α, β-unsaturated carbonyl system that assumes linear or nearly planar structure (Awasthi et al. 2009). Compounds of this category show a large variety of biological activity, together with antibacterial (Tran et al. 2012), malignant tumor (Syam et al. 2012; Kumar et al. 2014; Lawrence et al. 2006) anti-fungal, anti-inflammatory (Fang et al. 2014; Nowakowska et al. 2008), antiprotozoal drug, and antitubercular activities (Elias et al. 1999). The observation states that once electron-rich naphthyl rings are a gift in chalcones, they will participate in π–π interaction and image stacking interactions, and this could play a significant role in dimensioning inhibitors among the active sites of the enzymes (Girisha et al. 2017). There are different elements of an inflammatory reaction that will contribute to the associated symptoms and tissue injury. Edema, leukocytes infiltration, and tumor formation represent such components of inflammation. The purpose that chalcone hydrocarbon ring may be used as a valuable moiety within the definition of the latest malignant tumor

✉ Shankar Jayarama  
sankkar.bio@gmail.com

<sup>1</sup> PG Department of Biotechnology, Teresian College, Siddhartha Nagara, Mysuru, Karnataka 570011, India

specialists in numerous human cancers. In recent years, various naphthalene subordinates have been accounted to show anticancer action by repressing tubulin polymerization (Maya et al. 2005; Rasolofonjatovo et al. 2012). For the synthesis of compounds d1, the Claisen–Schmidt condensation reactions between equimolar quantities of 2-acetylnaphthalene and the appropriate aldehyde in the presence of aqueous sodium hydroxide solution were used to synthesize novel naphthalene containing chalcone were shown in Scheme 1. Prompted by these considerations, we have synthesized and characterization of chalcone containing two naphthyl substituents.

## Materials and methods

### Experimental section

The reaction mixture was monitored by TLC, performed on silica gel glass plates containing and visualization on TLC was achieved by U.V. light or iodine indicator. <sup>1</sup>H and <sup>13</sup>C NMR spectra were recorded on VNMRS-400 “Agilent–NMR” instrument. Chemical shifts (δ) are reported in ppm downfield from internal TMS standard, with tetramethylsilane (TMS) as the inside standard in DMSO as dissolvable.

### <sup>1</sup>H NMR and <sup>13</sup>C NMR

(2E)-3-(2-bromo-6-hydroxy-4-methoxyphenyl)-1-(naphthalene-2-yl) prop-2-en-1-one. Yield 81.92%, Yellow powder, m.p 162–164 °C, <sup>1</sup>H NMR (400 MHz, DMSO-d<sub>6</sub>): δ (ppm) 8.58 (s, 1H), 8.17–7.89 (m, 6H), 7.60–7.57 (m, 2H), 6.99–6.97 (d, J = 7.6, 1H), 6.47–6.45 (d, J = 6.8, 1H), 5.96–5.92 (t, J = 7.6, 1H), 3.61 (s, 3H) <sup>13</sup>C NMR 153.441, 146.708, 137.913, 134.741, 132.853, 129.632, 129.643, 126.563, 128.281, 127.999, 126.967, 125.002, 123.455, 121.402, 112.306, 111.595, 107.198.

### Cell lines and chemicals

The human malignant growth cell lines MCF-7, MDA-MB-231 (breast adenocarcinoma), HeLa (cervical cancer), HT-29, and HCT 116, (Colorectal adenocarcinoma) were got from the National Center for Cell Science, Pune, India. Cells were developed in suitable media enhanced with 10%

warmth inactivated Fetal Bovine Serum (FBS), 100 U/mL of penicillin, and 100 µg of streptomycin/mL, and brooded at 37 °C in a the humidified environment with 5% CO<sub>2</sub>. MTT [3-(4, 5-dimethylthiazol-2-yl)-2, 5-diphenyl tetrazolium bromide] was got from Sigma Chemicals.

### MTT cell viability assay

The cytotoxic movement of the mixes was resolved to utilize the MTT assay (Kamal et al. 2012). ( $1 \times 10^4$  cells/well) were seeded in 100 µl DMEM, enhanced with 10% FBS in each well of 96-well micro-culture plates and hatched for 24 h at 37 °C in a CO<sub>2</sub>. Mixes weakened with the predefined focus in the medium and added to the well. Following 48 h of brooding, 10 µl MTT (3-(4, 5-dimethylthiazol-2-yl)-2,5 diphenyl tetrazolium bromide) (5 mg/mL) was added to each well, and the plates were additionally incubated for 4 h. At that point, the supernatant from each well was cautiously removed, formazan precious stones were broken up in 100 µl of DMSO, and absorbance at 540 nm wavelength was recorded.

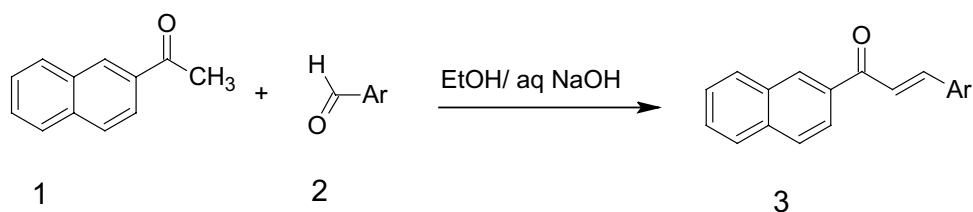
### Acridine orange/ethidium bromide staining

Nuclear staining was performed by utilizing the AO/EB double staining method. The MCF7 cells were collected from both the control and d1 treated groups. The cells were spread on clean glass slides and fixed in a fixative arrangement [methanol:acidic acid (3:1)]. The slides were hydrated with PBS and stained with Acridine orange/Ethidium bromide (1:1). The cells were thoroughly washed with PBS, observed under a fluorescent the magnifying instrument with a wavelength of 400–500 nm.

### RT-PCR

A semi-quantitative reverse transcriptase-polymerase chain reaction (RT-PCR) was carried out using the Techno Prime system to determine the levels of Caspase 9, Caspase 3, Bax, Bcl2, and β-Actin RNA expressions. The cDNA was synthesized from 2 µg of RNA using the Verso cDNA synthesis kit (Thermo Fischer Scientific) with an oligo dT primer as per the manufacturer’s instructions. The reaction volume was set to 20 µl, and cDNA synthesis was performed at 42 °C for 60 min, followed by R.T. inactivation at 85 °C for 5 min.

**Scheme 1** For the synthesis of compound d1, an aqueous sodium hydroxide solution (50% w/v, 5 ml) was added to equimolar mixtures (0.58 mmol of each component) of 2-acetylnaphthalene and the appropriate aldehyde



The reaction products of the samples were analyzed in 1.5% agarose gel.

## In vivo studies

### Animal and ethical statement

Swiss albino, BALB/c female mice, 6–8 week old weighing  $26 \pm 1.5$  g were housed under standard conditions and fed with animal chow and water were used all through the analysis. The mice were kept at room temperature ( $22 \text{ }^\circ\text{C} \pm 2 \text{ }^\circ\text{C}$ ) with proper ventilation for a 12 h day/night cycle. All animal experiments were endorsed by the Institutional Animal Ethics Committee (IAEC), (Approval No: BCP/IAEC/EXTP/05/2018) Bharathi College of Pharmacy, Bharathi Nagara, Mandya District, India.

### In vivo tumor model studies

The Ehrlich Ascites Tumor (EAT) cell lines were kept by the in vivo section. Tumors from the EAT-bearing Swiss albino mice were dissected under aseptic conditions. The cell suspension was made in 0.9% normal saline from the analyzed tumor. These EAT cells were infused intraperitoneally ( $5 \times 10^6$  cells/mouse) and were developed in the mice peritoneum developing ascites volume with stomach swelling. The animals demonstrated a sensational increment in body weight during the development period, and the animal sacrificed to the tumor trouble 10–12 days after implantation. The number of cells expanded during 10 days of development with an accumulation of 16–18 mL of ascites liquid with broad neovascularization in the internal coating of the peritoneal wall.

### Examination of body weight and collection of ascites fluid

To decide the effect of d1 against tumor development and angiogenesis, d1 (20 mg/kg body weight) was infused into EAT-bearing mice. After the sixth day of tumor transplantation development of the tumor was checked by taking the bodyweight of the experimental animals. The animals were sacrificed on the 12th day and ascites liquid was collected by making a small hole in the stomach area. EAT cells were segregated from ascites liquid as described earlier (Gururaj et al. 2002). Ascites liquid was collected from the animals and centrifuged at 3000 rpm for 10 min. EAT cells were obtained as a pellet, which were utilized for further examination. Ascites liquid volume was measured after separating from tumor cells.

## Peritoneal angiogenesis

The sacrificed mice were cut open at the midriff, and the internal covering of the peritoneal pit was opened to know about the impact of d1 on angiogenesis. Peritoneal depression of control and treated mice was taken.

### In ova chorioallantoic membrane (CAM) assay

The recombinant VEGF165 (rVEGF165) incited In Ova CAM angiogenesis models were used to explain the counter angiogenic impact of d1 in treated eggs as explained in the earlier technique (Hegde et al. 2012). Changes in the neo-angiogenesis design were analyzed and photographed using a Nikon digital camera.

### H and E staining analysis

Tissue segmenting of the liver, kidney, and the spleen, from the normal, Control, and the d1 treated mice was gathered and handled according to the standard convention (Penninger and Kroemer 2003a, b). Quickly, the tissues were implanted in paraffin wax, separated at 10 mm in a rotational a microtome (Leica Biosystems), and staining with hematoxylin and eosin. The magnifying lens assessed each segment with an appended CCD camera, and pictures were shot to compare the toxicity of the organs treated with d1 with that of the Control and normal mice organs.

## Results and discussion

### Chemistry

In the present study, synthesis was done of a series of naphthalene chalcones by the Claisen–Schmidt condensation reaction between equimolar quantities of 2-acetylnaphthalene and the appropriate aldehyde in the presence of aqueous sodium hydroxide solution. Column chromatography purified the synthesized compounds and was characterized by the LCMS, HPLC, and proton NMR spectroscopy. The appearance of two peaks around 7.4–7.2 ppm in the proton NMR spectrum confirms the formation of chalcone. The results also correlated with the formation of  $^{13}\text{C}$  NMR peaks at 110–120 ppm of chalcone.

### The cytotoxic examination and acridine orange and ethidium bromide assay

All the synthesized compounds were evaluated for their cytotoxic activity for various human cancer cell lines including MBA-MB-231, MCF-7 (breast adenocarcinoma), HeLa (cervical cancer), HT-29, and HCT 116 (Colorectal

adenocarcinoma) by MTT assay. The MTT is tetrazolium salt which gets reduced to formazan crystals. The intensity of formazan formed is a direct measure of the viability of the cells. The compound d1 exhibits potent anticancer activity with an  $IC_{50}$  estimation of  $8.15 \mu\text{M}$  concentration. Acridine orange is a vital dye and stains both live and dead cells. The cell treated with a given sample at various concentrations has shown a marked increase in apoptosis as the treatment concentration is increased. The results suggest that at  $8.15 \mu\text{M}$  treatment, the samples induced early apoptosis with cell membrane damage (Fig. 1a).

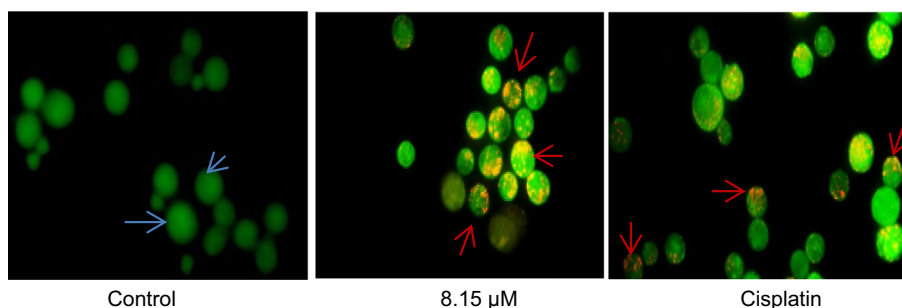
### Evaluation of the impact of d1 on Caspases 3 actuation in MCF7 cell line

In the evaluation of the effect of d1 chalcone on Bax, Bcl-2, and Caspases 3 initiations in MCF7 cell line, apoptotic pathway has been depicted as an essential for demise for mammalian cells (Rozmer and Perjési 2016). It is reported that activating Caspase-9 causes the activation of effector Caspases 3 in the apoptosis of the intrinsic pathway. Likewise, an expansion of the proapoptotic Bax expression and down-regulation of the counter apoptotic Bcl-2 (Naseri et al. 2015; Green and Reed 1998) is also observed. The definite proportion of Bax/Bcl-2 is necessary for the apoptosis acceptance by the mitochondrial pathway (Antonsson et al. 1997). It has been reported that chalcones initiate cell demise through apoptotic pathways as for example; the MCF7 cells treated with synthesized chalcone prompted apoptosis through the mitochondrial pathway and activated Caspase-3, while MCF7 cells can diminish the counter apoptotic of quality Bcl-2 and increase the level of an apoptotic gene. This persuaded us to take a view of the impact of the day 1 chalcones on the level of Bax/Bcl-2 and Caspase 3 activation on MCF7 cells. The outcome demonstrated that d1 hindered Bcl-2 and expanded Bax transcripts in MCF7 cells (Fig. 2), and showed a reasonable increment in Caspase 3 initiation when compared with the control (Fig. 2), proposing that d1 causes cell death by the mitochondrial apoptotic pathway.

### Compound d1 exhibits a potent antitumor effect on EAC model

We screened five different compounds in five different cell lines in that, we got good results in an MDA-MB-231 cell line (mammary carcinoma), and hence, based on the in vitro studies, we selected the EAC model (murine mammary adenocarcinoma) [Jaganathan and Mandal (2010) and Rai et al. (2016)]; hence, we selected EAC animal model for the in vivo studies to correlate the in vitro studies with animal models to correlate with mammary origin cancer. We have selected the EAC model based on mammary origin, and hence, it will be a suitable combination for the anticancer activity. The antitumor impact of d1 was further evidenced in in vivo tumor models. EAC tumor shows that d1 (20 mg/kg of three treatments) steadily diminishes the tumor cell expansion up to 80% (Fig. 3a). A diminished tumor volume appears to decrease in discharge of ascites volume to 2.1 ml in the treated mice when compared with the untreated control mice which are having 18 ml. Furthermore, the cell count number is synergized with tumor volume, and ascites emission enhances the cytotoxic impact of d1 (Fig. 3a–d). The antitumor action has simultaneously affected the survivability of the EAC-bearing mice, which has increased the survival time from 10 to 45 days (Fig. 3d). Angiogenesis was apparent in the internal peritoneal covering of EAC-bearing mice, and it is evidenced by the in vivo angiogenesis. Subsequently, the peritoneal covering of d1 treated mice was checked for its impact on peritoneal angiogenesis. The d1 addressed EAC-bearing tumor mice which demonstrated diminished peritoneal angiogenesis when compared with untreated mice (Fig. 3e). As against the angiogenic trademark, movement of d1 was all the while evaluated by utilizing the rVEGF165 incited CAM measure. The d1 inhibits the neovasculature (improvement in fresh recruit's vessels) in the newly developing embryos up to 75%, compared to Control and normal in vivo, as evident from the zone of vascularization (Fig. 3f).

**Fig. 1** Apoptosis inducing activity of d1 by AO/EB staining in MCF7 in with  $8.15 \mu\text{M}$  along with cisplatin (blue arrows indicate healthy morphology, whereas red indicate apoptotic cells)



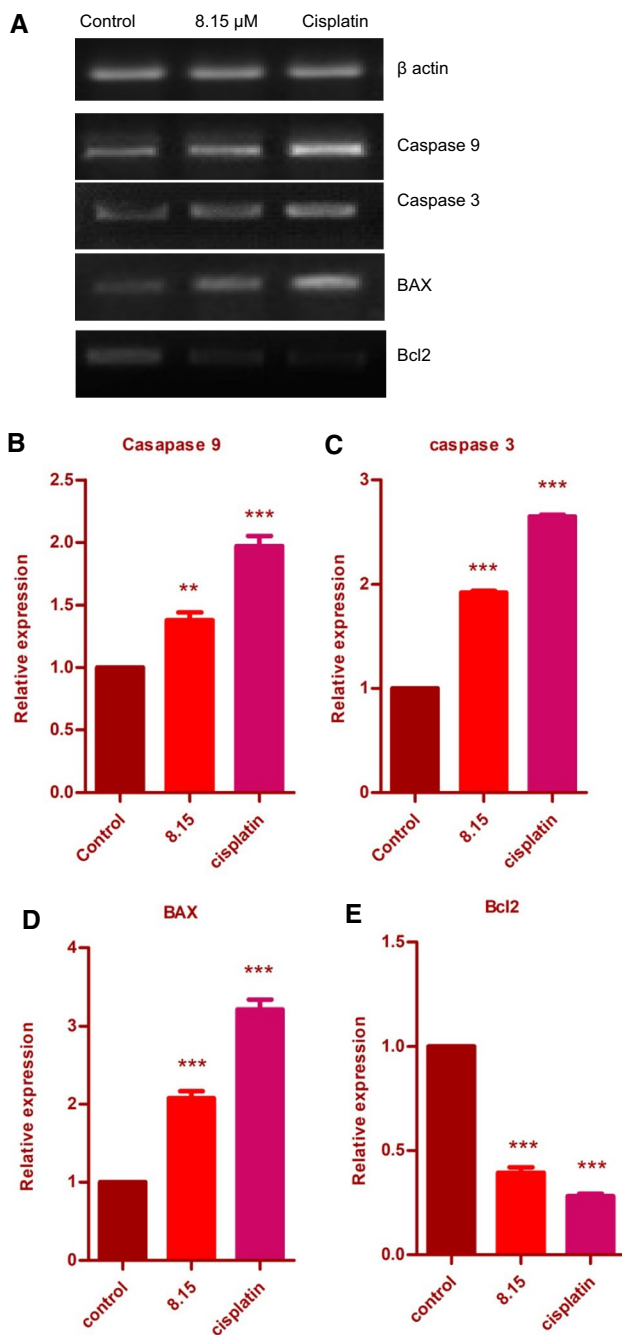


**Fig. 2** a Effect of d1 on mRNA expression levels of Bcl-2, Bax, and Caspase 3 and Caspase 9 in MCF7 cells after 48 h treatment.  $\beta$  actin was used as an internal control. b The relative gene expression of BAX, Bcl2, and Caspase 3 in treated MCF7 along with positive control cisplatin. Statistical significance are expressed as \* $p < 0.05$ , \*\* $p < 0.001$ , \*\*\* $p < 0.0001$  using One-way ANOVA

## Histopathological studies

As toxicological appraisal, the gross morphology of the analyzed inward organs of the typical, untreated Control, and treated EAC tumor-bearing mice was investigated. Because

of this strangely developed liver, kidney, and spleen in the control EAC tumor-bearing mice as compared with the treated EAC mice increased to a normal condition (Fig. 4). The outcome demonstrated that d1 administrated ordinary mice did not appear to have caused any complexity. The EAC-treated mice held practically a typical hematological profile, compared with the control mice. Histopathological studies included internal organs examination of the liver, kidney, and spleen. Normal spleen shows normal histology with well-placed white and red pulp areas. Seen are normally situated lymphoid follicles admixed with splenic sinusoids and entrapped a few erythrocytes. Control spleen shows distorted splenic sinusoids with admixed areas of passive congestion. Seen are foci of fibrosis and increased capsular thickness with sinusoidal dilatation. Treated spleen shows predominantly normal splenic histology with admixed areas of congestion and fibrosis. Splenic sinusoids show normal histology with admixed areas of hemorrhage. Cisplatin-treated mice show normal splenic histology with admixed areas of mild fibrosis and hemorrhagic areas. Sinusoidal space is normal with occasional foci of entrapped RBCs.

**Normal liver:** It shows normal hepatocytic lobular morphology with normally oriented central vein and portal triad. Lobular morphology, along with sinusoidal space, shows normal morphology with hepatocytes showing unremarkable changes. Control liver shows mild-to-moderate distortion of hepatic lobule with admixed areas of disrupted central vein and portal triad. Seen are areas of mild fibrosis and degeneration involving a few hepatocytes with congestive areas intervening. Treated liver shows predominantly normal hepatocytic morphology. Cisplatin-treated mice show normal hepatocytic histology with a few areas of congestion. Seen are normally oriented central vein and portal triad with no degenerative zones. Normal kidney sections studied show normal glomerular and tubular differentiation. Seen are normal histology of glomeruli with capillary tufting and tubules with normal lining.

**Control kidney:** Sections studied show mild-to-moderate distortion of glomeruli and tubular architecture. Glomeruli at places show atrophic changes with admixed chronic inflammatory cells. Tubules show increased thickening of lining cells. The d1 treated sections studied show predominantly normal histology of glomeruli and tubules. Seen are a few foci of chronic inflammatory cells admixed with glomeruli showing distorted morphology. Cisplatin-treated mice: Tubules show normal histology. Sections studied show normal histology with mildly distorted glomeruli at places. Normal tubular and stromal morphology was seen (Fig. 4).

In the present examination, we illustrated the counter angiogenic movement of d1 by performing both in vivo and in vitro angiogenesis tests. We saw that d1 treatment essentially restrained the improvement of capillary development in CAM. The d1 treatment did not demonstrate any cytotoxicity

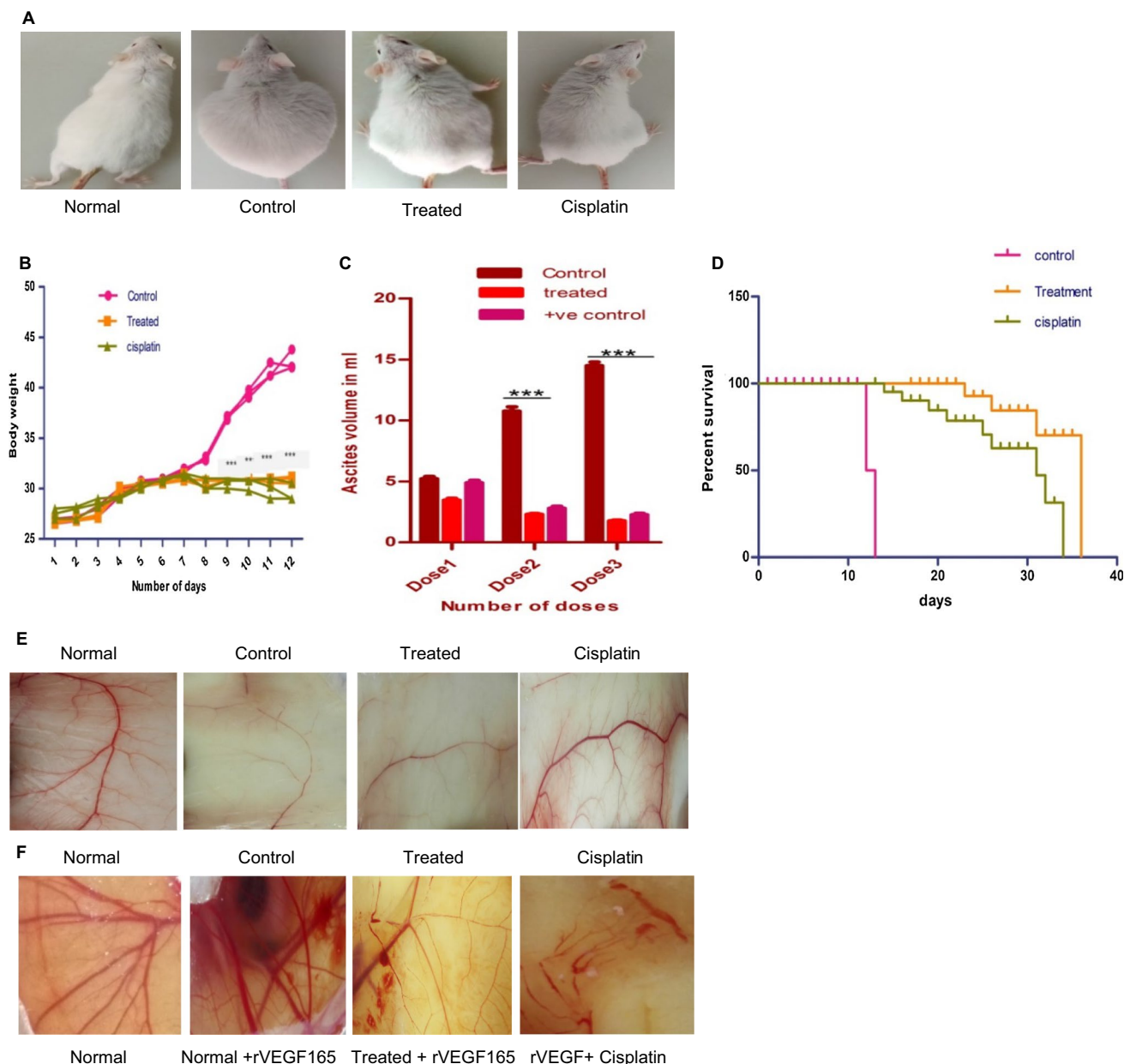


**Fig. 3** The d1 diminishes the expansion of the Ehrlich Ascites Carcinoma shows in vivo. EAC cells were cultured in vivo and directed with 20 mg/kg b.w. (i.p.) of d1 of three dosages and tumor, and factors were examined. **a** Morphological changes of EAC tumor-bearing mice after treatment. **b** Decreases the bodyweight of EAC tumor-bearing mice. **c** There is a diminishing in ascites liquid discharge. **d** Tumorigenic record is characteristic of the level of decrease in tumor development. The Kaplan–Meier chart bend demonstrates the all-encompassing survivability of d1 treated mice. The outcomes are

the methods for three judgments, each directed in triplicate. **e** The d1 declines the tumoral neovascularization in EAC tumor-bearing mice in vivo: The impact of d1 in a tumor initiated angiogenesis was inspected by EAC tumor-bearing mice treated with d1 20 mg/kg body weight i.p. **a** The peritoneal covering of mice demonstrates the noticeable concealment of peritoneal angiogenesis in d1 treated when contrasted with Control. **f** In vivo CAM photos appearing decreased degree of rVEGF165 initiated angiogenesis. Statistical significance was expressed as  $*p < 0.05$ ;  $**p < 0.001$ ;  $***p < 0.0001$

in 8.15  $\mu\text{M}$  concentration. At this scope of focus, we saw that d1 inhibited the expansion of angiogenesis. As per the information got from both in vivo and in vitro angiogenesis measures, we reasoned that d1 has a robust enemy of angiogenic impact on these consecutive angiogenic cascades.

VEGF is outstanding as an essential nutrient for angiogenesis. Tests were also done to know whether these components were engaged with the counter angiogenic action of d1 and the outflow of angiogenesis in the EAC model and chick embryo through peritoneal angiogenesis and CAM assay.

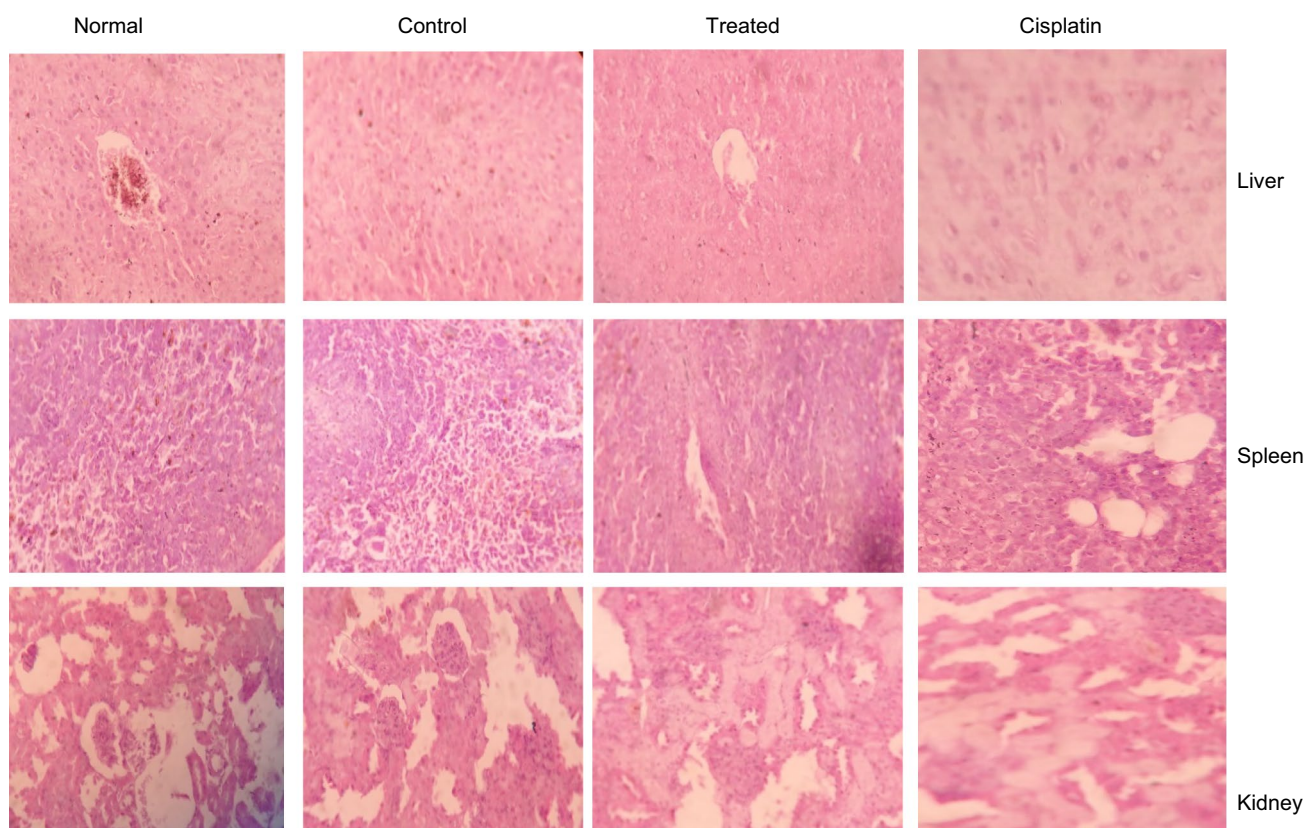


**Fig. 4** The toxicology studies for d1 in EAC models for liver, spleen, and kidney

This information may direct is to know the possibility that d1 may regulate the statements of different angiogenesis-related qualities. The report got from in vivo and in vitro angiogenesis examines proposes that d1 has a strong inhibiting capability of angiogenic movement. This inhibiting angiogenic action of d1 in vivo and in vitro encouraged us to inspect the apoptosis-prompting progress of d1 in MCF7 cells. This information suggests that d1 induced cell death through the apoptotic process in MCF7 cells. Caspases can be predicted as the focal killers of the apoptotic pathway, since they initiate a large portion of the noticeable changes that caused apoptotic cell demise. The apoptotic pathway has been described as an essential signaling of cell death for mammalian cells. The results showed that d1 activated Caspase 3 in MCF7 cells and showed an apparent increase in Caspase 3 activation.

Our investigation firmly proposes that d1 is the enemy of angiogenic impact on endothelial cells, yet additionally apoptosis-activating action on tumor cells. From the above, it is suggested that d1 is confirming the multi-powerful enemy of cancerous growth. In d1, the methoxy group showed a significant activity in anticancer studies. Electron-donating groups make the compound electron-rich, and continuous resonance is possible, which makes efficient bonding.

### Statistical analysis

Statistical analysis was performed by One-way and One-way ANOVA accompanied by Bonferroni's Multiple Comparison Test and "Dunnett's Multiple Comparison Test" was used to analyze comparisons;  $p < 0.05$  was considered to indicate a significant difference for calculating  $IC_{50}$  of all the compounds. Data were analyzed using Graph Pad Prism 5.0 software.

### Conclusion

In the present study, a series of naphthalene chalcone were synthesized by the Claisen condensation and carried out the anti-angiogenic and proapoptotic activity studies, and the results show that compound with an electron-donating group exhibits the superior activity in this compound.

**Acknowledgements** This study was supported and funded by Rajiv Gandhi National Fellowship (RGNF-UGC); ORDER NO. SPC/43/RGNF/2013-14. P.G. Department of Biotechnology Teresian College, Mysuru; and the Department of the chemistry University of Mysore. The authors acknowledge the Teresian Research Foundation and P.G.

Department of Biotechnology, Teresian College (affiliated to the University of Mysore) for providing animal cell culture facility. The authors would like to thank the Department of Pharmacy, Bharathi College of Pharmacy, KM Doddi, Mandya, and Karnataka for providing the animal house facility.

**Author contributions** The biological activity, synthesis, and characterizations were carried out by DKMG. The research supervisor is SJ.

## Compliance with ethical standards

**Conflict of interest** The authors reported no potential conflict of interest.

## References

- Antonsson B, Conti F, Ciavatta A, Montessuit S, Lewis S, Martinou I, Bernasconi L, Bernard A, Mermod JJ, Mazzei G, Maundrell K (1997) Inhibition of Bax channel-forming activity by Bcl-2. *Science* 277:324:370–372. <https://doi.org/10.1126/science.277.5324.370>
- Awasthi SK, Mishra N, Kumar B, Sharma M, Bhattacharya A, Mishra LC, Bhasin VK (2009) potent antimalarial activity of newly synthesized substituted chalcone analogs in vitro. *Med Chem Res* 6:407–420. <https://doi.org/10.1007/s00044-008-9137-9>
- Cragg GM, Newman DJ (2013) Natural products: a continuing source of new drug leads. *Biochimica et Biophysica Acta (BBA)*. <https://doi.org/10.1016/j.bbagen.2013.02.008>
- Elias DW, Beazely MA, Kandepe NM (1999) Bioactivities of chalcones. *Curr Med Chem* 12:1125. [https://doi.org/10.1016/S0024-3205\(00\)00974-7](https://doi.org/10.1016/S0024-3205(00)00974-7)
- Fang Q, Zhao L, Wang Y, Zhang Y, Li Z, Pan Y, Kanchana K, Wang J, Tong C, Li D, Liang G (2014) A novel chalcone derivative attenuates the diabetes-induced renal injury via inhibition of high glucose-mediated inflammatory response and macrophage infiltration. *Toxicol Appl Pharmacol* 2:129–138. <https://doi.org/10.1016/j.taap.2014.10.021>
- Girisha M, Sagar BK, Yathirajan HS, Rathore RS, Glidewell C (2017) Three closely related 1-(naphthalene-2-yl) prop-2-en-1-ones: pseudosymmetry, disorder and supramolecular assembly mediated by C—H... $\pi$  and C—Br... $\pi$  interactions. *Acta Crystallogr Sect C: Struct Chem* 2:115–120. <https://doi.org/10.1107/S205322961700105X>
- Green DR, Reed JC (1998) Mitochondria and apoptosis. *Science* 281:1309–1312. <https://doi.org/10.1126/science.281.5381.1309>
- Gururaj AE, Belakavadi M, Venkatesh DA, Marmé D, Salimath BP (2002) Molecular mechanisms of the antiangiogenic effect of curcumin. *Biochem Biophys Res Commun* 4:934–942. [https://doi.org/10.1016/S0006-291X\(02\)02306-9](https://doi.org/10.1016/S0006-291X(02)02306-9)
- Hegde M, Karki SS, Thomas E, Kumar S, Panjamurthy K, Ranganatha SR, Rangappa KS, Choudhary B, Raghavan SC (2012) New levamisole derivative induces the extrinsic pathway of apoptosis in cancer cells and inhibits tumor progression in mice. *PLoS One* 9:e43632. <https://doi.org/10.1371/journal.pone.0043632>
- Jaganathan SK, Mandal M (2010) Involvement of non-protein thiols, mitochondrial dysfunction, reactive oxygen species and p53 in honey-induced apoptosis. *Invest New Drugs* 28(5):624–633. <https://doi.org/10.1007/s10637-009-9302-0>
- Kamal A, Mallareddy A, Suresh P, Nayak VL, Shetti RV, Rao NS, Tamboli JR, Shaik TB, Vishnuvardhan MV, Ramakrishna S (2012) Synthesis and anticancer activity of 4 $\beta$ -alkylamidochalcone and 4 $\beta$ -cinnamido linked podophylotoxins as apoptotic inducing agents. *Eur J Med Chem* 47:530–545. <https://doi.org/10.1016/j.ejmech.2011.11.024>
- Kumar D, Kumar NM, Tantak MP, Ogura M, Kusaka E, Ito T (2014) Synthesis and identification of  $\alpha$ -cyano bis (indolyl) chalcones as novel anticancer agents. *Bioorg Med Chem Lett* 22:5170–5174. <https://doi.org/10.1016/j.bmcl.2014.09.085>
- Lawrence JJ, Grinspan ZM, Statland JM, McBain CJ (2006) Muscarinic receptor activation tunes mouse stratum oriens interneurons to amplify spike reliability. *J Physiol* 3:555–562. <https://doi.org/10.1113/jphysiol.2005.103218>
- Maya AB, Pérez-Melero C, Mateo C, Alonso D, Fernández JL, Gajate C, Mollinedo F, Peláez R, Caballero E, Medarde M (2005) Further naphthylcombretastatins. An investigation on the role of the naphthalene moiety. *J Med Chem* 2:556–568. <https://doi.org/10.1021/jm0310737>
- Mishra BB, Tiwari VK (2011) Natural products: an evolving role in future drug discovery. *Eur J Med Chem* 10:4769–4807. <https://doi.org/10.1016/j.ejmech.2011.07.057>
- Naseri MH, Mahdavi M, Davoodi J, Tackallou SH, Goudarzvand M, Neishabouri SH (2015) The up-regulation of Bax and down-regulation of Bcl2 during 3-NC mediated apoptosis in human cancer cells. *Cancer Cell Int* 1:55. <https://doi.org/10.1186/s12935-015-0204-2>
- Newman DJ, Cragg GM (2016) Natural products as sources of new drugs from 1981 to 2014. *J Nat Prod* 3:629–661. <https://doi.org/10.1021/acs.jnatprod.5b01055>
- Nowakowska Z, Kędzia B, Schroeder G (2008) Synthesis, physicochemical properties, and antimicrobial evaluation of new (E)-chalcones. *Eur J Med Chem* 4:707–713. <https://doi.org/10.1016/j.ejmech.2007.05.006>
- Partridge E, Gareiss P, Kinch MS, Hoyer D (2016) An analysis of FDA-approved drugs: natural products and their derivatives. *Drug Discov Today* 2:204–207. <https://doi.org/10.1016/j.drudis.2015.01.009>
- Penninger JM, Kroemer G (2003a) Mitochondria, AIF, and caspases—rivaling for cell death execution. *Nat Cell Biol* 2:97
- Penninger JM, Kroemer G (2003b) Mitochondria, AIF and caspases—rivaling for cell death execution. *Nat Cell Biol* 5(2):97–99. <https://doi.org/10.1038/ncb0203-97>
- Rai G, Mishra S, Suman S, Shukla Y (2016) Resveratrol improves the anticancer effects of doxorubicin in vitro and in vivo models: a mechanistic insight. *Phytomedicine* 23(3):233–242. <https://doi.org/10.1016/j.phymed.2015.12.020>
- Rasolofonjatovo E, Provot O, Hamze A, Rodrigo J, Bignon J, Wdzieczak-Bakala J, Desravines D, Dubois J, Brion JD, Alami M (2012) Conformationally restricted naphthalene derivatives type is combretastatin A-4 and isoeberianin analogs: synthesis, cytotoxicity and ant tubulin activity. *Eur J Med Chem* 52:22–32. <https://doi.org/10.1016/j.ejmech.2012.12.042>
- Rodrigues T, Reker D, Schneider P, Schneider G (2016a) Counting on natural products for drug design. *Nat Chem* 6:531
- Rodrigues T, Reker D, Schneider P, Schneider G (2016b) Counting on natural products for drug design. *Nat Chem* 8(6):531–541. <https://doi.org/10.1038/nchem.2479>
- Rozmer Z, Perjési P (2016) Naturally occurring chalcones and their biological activities. *Phytochem Rev* 1:87–120. <https://doi.org/10.1007/s11101-014-9387-8>
- Syam S, Abdelwahab SI, Al-Mamary MA, Mohan S (2012) Synthesis of chalcones with anticancer activities. *Molecules* 6:179–195. <https://doi.org/10.3390/molecules17066179>
- Tran TD, Nguyen TT, Do TH, Huynh TN, Tran CD, Thai KM (2012) Synthesis and antibacterial activity of some heterocyclic chalcone analogs alone and in combination with antibiotics. *Molecules* 6:6684–6696. <https://doi.org/10.3390/molecules17066684>



Warmka JK, Solberg EL, Zeliadt NA, Srinivasan B, Charlson AT, Xing C, Wattenberg EV (2012) the inhibition of mitogen-activated protein kinases increases the sensitivity of A549 lung cancer cells to the cytotoxicity induced by a kava chalcone analog. *Biochem Biophys Res Commun* 3:488–492. <https://doi.org/10.1016/j.bbrc.2012.06.140>

**Publisher's Note** Springer Nature remains neutral with regard to jurisdictional claims in published maps and institutional affiliations.